SUSTAINABLE DEVELOPMENT GOALS

Global Water Resources Data Products (2023 edition)

International Research Center of Big Data for Sustainable Development Goals
March 2023

Global Water Resources Data Products (2023 edition)

Preface

The United Nations 2030 Agenda for Sustainable Development has drawn an ambitious vision for global sustainable development in three dimensions: economic, social and environmental. However, it has faced grand challenges posed by issues including a lack of data, uneven progress, and trade-offs among the Sustainable Development Goals (SDGs). In response, the Decade of Action to deliver the SDGs by 2030, as one of the priorities for data action in the report on "Data Strategy of the Secretary General for Action by Everyone, Everywhere: With Insight, Impact and Integrity (2020-22)", has addressed the issue on "how to get more relevant, disaggregated and timely data to track, predict and accelerate SDG progress", which is expected to help turn data and information into insights to optimize and improve decision-making process on development issues.

On September 22, 2020, Chinese President Xi Jinping announced at the 75th Session of the UN General Assembly that China would establish the International Research Center of Big Data for Sustainable Development Goals (CBAS). The CBAS was officially inaugurated on September 6, 2021, and is the first international scientific institution in the world to harness Big Data in service of the 2030 Agenda. Since its inception, the CBAS has focused on seven SDGs in particular: Zero Hunger, Clean Water and Sanitation, Affordable and Clean Energy, Sustainable Cities and Communities, Climate Action, Life Below Water, and Life on Land, and has dynamically assessed global progress on the relevant SDG indicators. The CBAS has built the SDG Big Data Platform, developed and launched the SDGSAT-1 satellite, and provides integrated big data services to the world to advance sustainable development. The CBAS is committed to developing theoretical and technical methods for the applications of Big Earth Data for sustainable development assessment, conducting research on the monitoring and evaluation of global sustainable development indicators, sharing cutting-edge methods and successful practices, and constantly making scientific proposals on how Big Data can promote the realization of the SDGs.

In September 2022, the set of Global Sustainable Development Data Products (including 6 products) were presented to the UN by Chinese government to provide data support for scientific decision-making on the SDGs. In February 2023, Csaba Kőrösi, President of the 77th Session of the UN General Assembly, visited the CBAS and spoke highly of the achievements of the CBAS in monitoring and evaluating progress toward the SDGs. He invited and expected the CBAS to share China's scientific knowledge and experience in the implementation and assessment of the SDG 6 and in the field of water resources in general.

The Global Water Resources Data Products (2023 edition) reflects the extensive and in-depth research conducted at the CBAS in the areas of drinking water safety, water quality improvement, water efficiency and the water-related ecosystems conservation, as well as the practice of assessing the progress toward SDG 6 at global and regional scales. It includes 7 datasets, such as global cropland water-use efficiency and the Forel-Ule Index of large lakes, among others. These products were created and validated using open data sources, and data disclosure is in line with international conventions on scientific data sharing in the field. It is expected to provide data support for understanding the sustainable use of global water resources, and contribute to the forthcoming Global Water Information System of the United Nations.

Director-General
International Research Center of Big Data for
Sustainable Development Goals

Global Water Resources Data Products (2023 edition)

CONTENTS

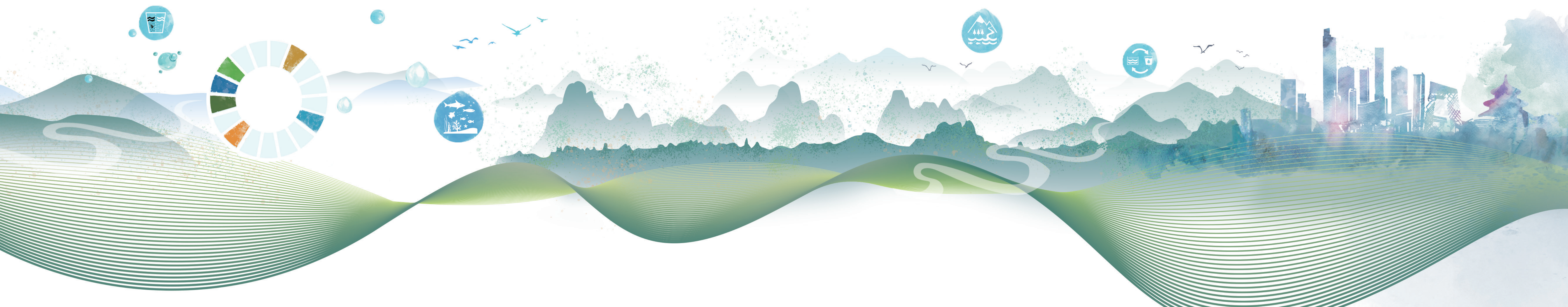

Global daily 1-km actual evapotranspiration from 2000 to 2021 (ETMonitor-1km_2000-2021)

Product summary

The evapotranspiration (ET) in this product refers to the actual land surface evapotranspiration (unit: mm), which is the sum of vegetation transpiration, canopy rainfall interception loss, soil evaporation, open water evaporation, and ice/snow sublimation. ET is an essential ecohydrological process that links the energy, water and carbon cycles of the land surface and plays a critical role in the Earth system. Accurate estimation of land surface ET is not only of great significance for the study of the water cycle and energy exchange processes of the Earth system, but is also valuable for applications in the effective management of water and land resources, monitoring of crop water requirements for irrigation scheduling, flood/drought monitoring and assessment for disaster management, and many others.

Temporal

The product covers the period 2000–2021, with a temporal resolution of 1 day.

Geo Scope

The product covers the geographical area between 90° N–90° S latitude and 180° W–180° E longitude, with a spatial resolution of 1km.

support SDGs

6 CLEAN WATER AND SANITATION

SDG 6.4.1 Change in water-use efficiency over time

SDG 6.4.2 Level of water stress: freshwater withdrawal as a proportion of available freshwater resources

SDG 6.6.1 Change in the extent of water-related ecosystems over time

Global land surface evapotranspiration at 1-km resolution in 2020

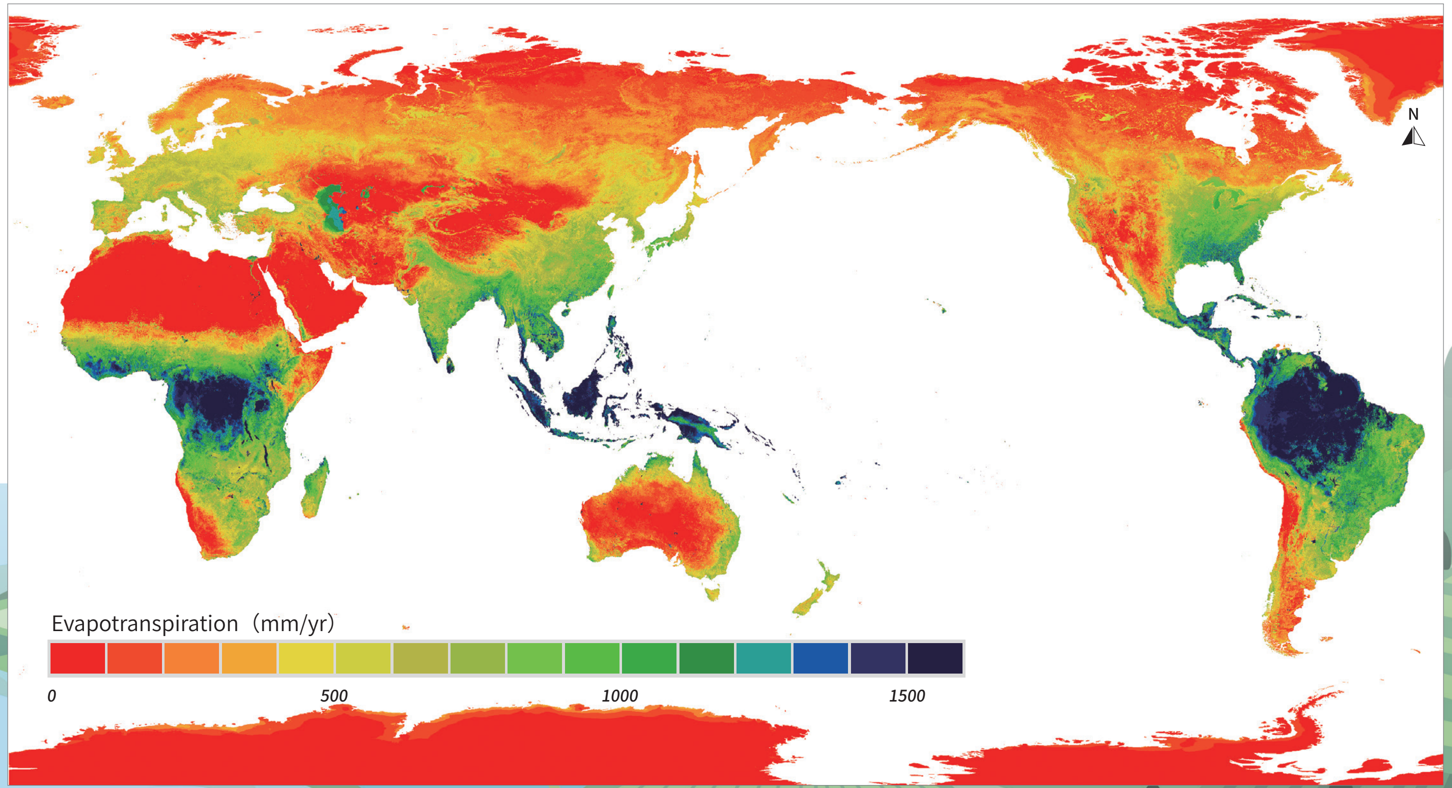

Methodology

This global ET dataset was obtained using the ETMonitor model, which was driven by multi-source satellite remote sensing data and reanalysis data (Zheng et al., 2022). The ETMonitor model established a multi-parameterization scheme for evapotranspiration components (vegetation transpiration, canopy rainfall interception loss, soil evaporation, water surface evaporation, snow and ice sublimation), taking into account the simulation of the energy balance, water balance and plant physiological processes that control the surface energy and water exchanges (Zheng & Jia, 2020; Hu & Jia, 2015). All the ET components of each remote sensing pixel were first estimated, and the total actual ET of each pixel was obtained by accumulating the ET components.

The input data include: (1) remote sensing data: Leaf Area Index, Fraction of Vegetation Cover and land surface Albedo from the Global LAnd Surface Satellite (GLASS) product; MODIS land cover/use classification data and snow cover data; FROM-GLC daily dynamic surface water cover data developed by Tsinghua University; ESA CCI soil moisture data from the European Space Agency; GPM precipitation data; (2) meteorological data: downward shortwave and longwave radiation, wind speed, air temperature and dew-point temperature provided by the ERA5 global reanalysis dataset.

The input data were rescaled to the daily 1-km resolution using time series analysis, machine learning and spatiotemporal conversion methods. Finally, the ETMonitor model was applied to these forcing data to estimate global ET at daily and 1-km resolution.

Accuracy assessment

The validation was conducted using flux observations from the 251 ground flux sites around the world, covering a wide range of terrestrial ecosystems as well as water and snow/ice surfaces. The validation result showed that the Root Mean Square Error (RMSE) of daily evapotranspiration of this product generated by the ETMonitor model was 0.93 mm/day.

Product format

This product uses the WGS84 coordinate system with latitude and longitude projection (EPSG: 4326). Data are stored in GeoTIFF format. Each file contains one data layer (band) of daily evapotranspiration over the land surface of the globe. The unit of the evapotranspiration in this product is mm/day, with a conversion factor of 0.01.

Analysis result

The analysis results showed that the global multi-year mean annual actual evapotranspiration was 72.59 (±1.44) × 10^3 km^3, and the spatial pattern of ET was highly related to the atmospheric moisture demand or land surface moisture supply. Annual ET gradually decreased with increasing latitude, corresponding to differences in climatic conditions, land cover types, and vegetation growing season lengths. In arid/semi-arid regions, high ET values occurred in irrigated croplands, e.g., Nile Delta, Indus Basin, Central Asian inland river basins, due to irrigation water supply. Global ET showed an overall increasing trend in 2000-2021, consistent with the global warming trend although significant spatial variation was observed. In general, the regions with increased ET correspond to regions with vegetation greening and cropland expansion, suggesting that these two factors could accelerate the water cycle. The regions with decreased ET were mainly associated with drought intensification and tropical rainforest disturbance (e.g., forest fires in the Amazon).

Dataset citations

Chaolei Zheng, Li Jia, Guangcheng Hu. Global daily 1-km actual evapotranspiration from 2000 to 2021 (ETMonitor-1km_2000-2021), Beijing: International Research Center of Big Data for Sustainable Development Goals (CBAS), 2023. doi: 10.12237/casearth.640f012a819aec3f2b52a4b6

References

Chaolei Zheng, Li Jia, Guangcheng Hu. 2022. Global Land Surface Evapotranspiration Monitoring by ETMonitor Model Driven by Multi-source Satellite Earth Observations. Journal of Hydrology, 613: 128444. https://doi.org/10.1016/j.jhydrol.2022.128444

Chaolei Zheng, Li Jia. 2020. Global canopy rainfall interception loss derived from satellite earth observations. Ecohydrology, 13(2): e2186. https://doi.org/10.1002/eco.2186

Guangcheng Hu, Li Jia. 2015. Monitoring of evapotranspiration in a semi-arid inland river basin by combining microwave and optical remote sensing observations. Remote Sensing, 7(3), 3056-3087. https://doi.org/10.3390/rs70303056

Product URL

http://data.casearth.cn/thematic/GWRD_2023

QR code

Contact information

Chaolei Zheng, Associate Professor, clzheng@cbas.ac.cn   Li Jia, Professor, lijia@cbas.ac.cn

Citation and Disclaimer for Data Use

Global daily 1-km actual evapotranspiration

Global 1-km cropland water-use efficiency from 2001 to 2020 (GCWUE-1km_2001-2020)

Product summary

The cropland water-use efficiency (WUE) defined in this product refers to the ratio between Net Primary Productivity (NPP) and Evapotranspiration (ET) of croplands (unit: g C · kg^{-1} H_2O · yr^{-1}). WUE characterizes the trade-off between photosynthetic carbon assimilation and water use, and reflects the capacity of cropland to provide ecosystem services. The cropland WUE is linked to human well-being and sustainable development goals, among other things. With limited water resources and increasing water demand, improving cropland WUE to reduce water consumption per unit of productivity is a critical way to mitigate global water scarcity.

Temporal

The product covers the period 2001–2020, with a temporal resolution of 1 year.

Geo Scope

The product covers the geographical area between 90° N–90° S latitude and 180° W–180° E longitude, with a spatial resolution of 1km.

support SDGs

6 CLEAN WATER AND SANITATION

SDG 6.4.1 Change in water-use efficiency over time

Global cropland water-use efficiency at 1-km resolution in 2020

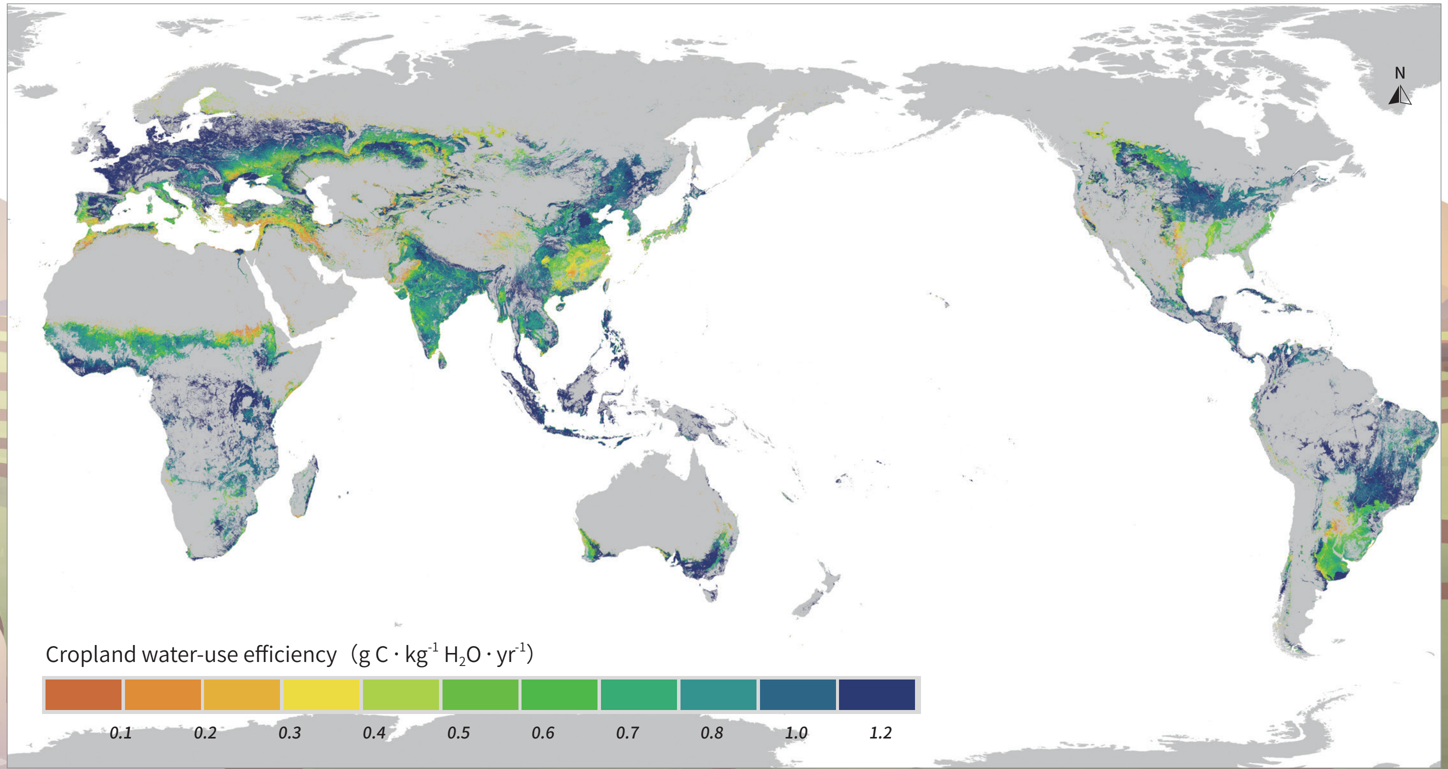

Methodology

Cropland water-use efficiency was calculated as the ratio of Net Primary Productivity (NPP) to evapotranspiration (ET). Cropland ET was from the "Global daily 1-km actual evapotranspiration from 2000 to 2021" dataset from this edition of data products. Cropland NPP is equal to Gross Primary Productivity (GPP) minus the fraction of the stored organic carbon consumed by crops to maintain crop respiration (CR). GPP was estimated using an improved Light Use Efficiency model (EF-LUE) (Du et al., 2022), which introduced a new parameterization to account for soil water stress, thus improving the accuracy of GPP estimation under water stress conditions. CR was obtained by summing the growth respiration (proportional to NPP) and maintenance respiration (related to Leaf Area Index).

Input data include (1) Fraction of Photosynthetically Active Radiation (fPAR) and Leaf Area Index from Global LAnd Surface Satellite (GLASS) product and (2) downward shortwave radiation, air and dew-point temperatures from ERA5 global reanalysis dataset. The global cropland distribution (i.e., pure cropland pixels and cropland/natural vegetation mosaic pixels) was obtained from the European Space Agency Climate Change Initiative (ESA-CCI) land cover/use classification data. Finally, the global cropland water-use efficiency product for 2001–2020 with an annual time step and a spatial resolution of 1-km was created using the aforementioned models, techniques and input data.

Accuracy assessment

The flux observations from the 21 global cropland ecosystem flux sites worldwide were used to obtain the site values of evapotranspiration and GPP, and the site NPP was obtained by combining the site GPP and the GLASS leaf area index data of the pixel of the corresponding sites (used to estimate crop maintenance respiration). Finally, the site values of cropland water-use efficiency were calculated and used as the "ground truth" data to validate the cropland WUE product. The validation result showed that the Root Mean Square Error (RMSE) of cropland water-use efficiency of this product was 0.5 $g\ C \cdot kg^{-1}\ H_2O \cdot yr^{-1}$.

Product format

This product uses the WGS84 coordinate system with latitude and longitude projection (EPSG: 4326). Data are stored in GeoTIFF format. Each file contains one data layer (band) of annual cropland water-use efficiency over croplands of the globe. The unit of water-use efficiency in this product is $g\ C \cdot kg^{-1}\ H_2O \cdot yr^{-1}$.

Analysis result

The result of the global spatial pattern of cropland water-use efficiency showed that the tropical regions had the highest values, followed by arid/semi-arid regions and cold regions, and relatively lower values in temperate regions. Trend analysis showed that cropland water-use efficiency increased globally from 2001 to 2020, but there was considerable spatial variability. The rise in cropland water-use efficiency higher in arid/semi-arid regions was because the increase in NPP outpaced the increase in evapotranspiration. The increase in cropland water-use efficiency was the smallest in cold regions because the increase in NPP was only slightly greater than the increase in evapotranspiration. Technological advances, such as field management, water-saving practices, breeding, and others—along with some degree of climate change—have boosted crop biomass, which has increased agricultural water-use efficiency.

Dataset citations

Min Jiang, Chaolei Zheng, Li Jia. Global 1-km cropland water-use efficiency from 2001 to 2020 (GCWUE-1km_2001-2020), Beijing: International Research Center of Big Data for Sustainable Development Goals (CBAS), 2023. doi: 10.12237/casearth.640f0132819aec3f2b52a4bb

References

Dandan Du, Chaolei Zheng, Li Jia, et al. 2022. Estimation of Global Cropland Gross Primary Production from Satellite Observations by Integrating Water Availability Variable in Light-Use-Efficiency Model. Remote Sensing, 14(7): 1722. https://doi.org/10.3390/rs14071722

Product URL

http://data.casearth.cn/thematic/GWRD_2023

QR code

Contact information

Min Jiang, Assistant Professor, minjiang@cbas.ac.cn Li Jia, Professor, lijia@cbas.ac.cn

Citation and Disclaimer for Data Use

Global 30-m annual maximum land surface water cover in 2000, 2005, 2010, 2015, 2021 (GAMLSW30)

Product summary

Global annual maximum land surface water cover refers to the maximum distribution of all types of water present on the land surface, derived from all available Landsat satellite data within the year. The distribution of global land surface water cover is strongly influenced by global change, and its changes have important implications for biodiversity and the health of water-related ecosystems.

Temporal

The product covers five time periods: 2000, 2005, 2010, 2015, 2021.

Geo Scope

The product covers the geographical area between 80° N–80° S latitude and 180° W–180° E longitude, with a spatial resolution of 30 meters.

support SDGs

- SDG 6.6.1 Change in the extent of water-related ecosystems over time
- SDG 15.1.2 Proportion of important sites for terrestrial and freshwater biodiversity that are covered by protected areas, by ecosystem type

Global 30-m annual maximum land surface water cover in 2021

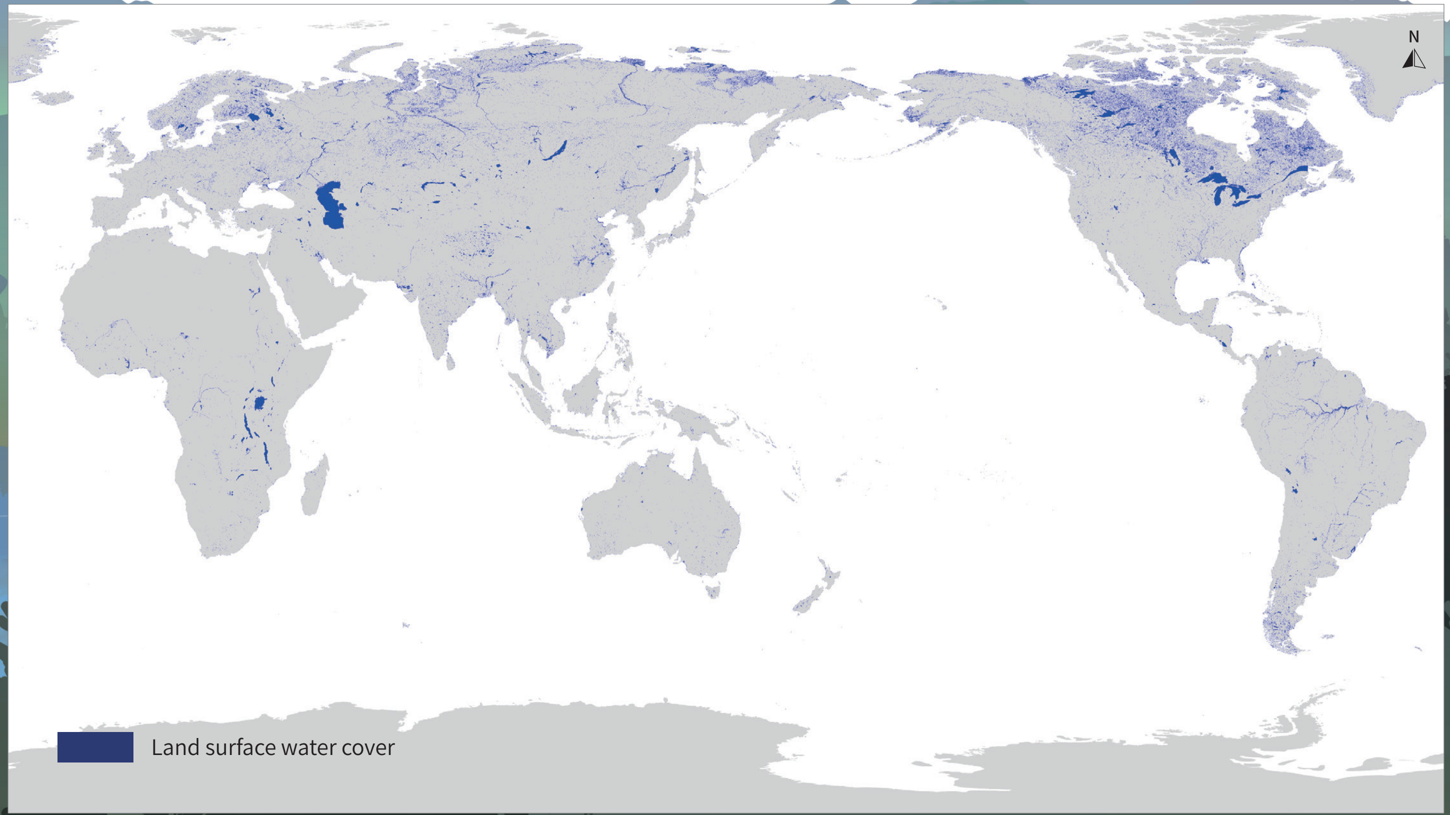

Methodology

The input data used to produce GAMLSW30 include Landsat data and Shuttle Radar Topography Mission (SRTM) Digital Elevation Model (DEM) data. Global Multi-resolution Terrain Elevation Data 2010 (GMTED2010) was used in high-latitude areas due to lack of SRTM-DEM data.

Firstly, an annual Landsat top-of-atmosphere reflectance dataset was created and cloud masking was applied. Feature indices such as the NDVI (Normalized Difference Vegetation Index), NDWI (Normalized Difference Water Index), and NDSI (Normalized Difference Snow Index) were calculated, while terrain indices were obtained from the DEM. Subsequently, a set of land surface water extraction rules based on multiple indices thresholds were established using prior knowledge (Liu et al., 2021). Finally, the land surface water extraction rules were applied to multi-temporal Landsat data of the same area within a year to extract land surface water cover, and the annual maximum land surface water cover product was generated by integration.

Accuracy assessment

Throughout the production of the dataset, whole-process quality control and random quality inspection were adopted to ensure the quality of the product. A total of 7028 land surface water verification points were uniformly selected globally to assess the accuracy of the dataset, and the overall accuracy was 90.6%.

Product format

This product uses the WGS84 geographic coordinate system and longitude and latitude projection (EPSG: 4326). The data are stored in GeoTIFF format. Each annual product contains 612 spatial tile files, each tile file having a spatial extent of 10° ×10° latitude and longitude (approximately 37000×37000 pixels). Each tile file contains a single layer (band), with a value of 1 for non-land surface water cover and a value of 2 for land surface water cover.

Analysis result

The analysis results showed that the maximum area of global land surface water cover in 2000, 2005, 2010, 2015, and 2021 was 3.69×10^6 km^2, 3.60×10^6 km^2, 3.58×10^6 km^2, 3.89×10^6 km^2 and 3.98×10^6 km^2, respectively, showing a fluctuating increasing trend. The area of land surface water cover in Africa, Asia, Europe, and North America showed a fluctuating increasing trend, but there were significant spatial differences. The lake agglomeration areas in North America and Asia were the main regions where the annual maximum water cover increased, while in Central Asia, the annual maximum water cover showed a fluctuating decrease. In South America, the annual maximum water cover remained stable. In Oceania, the annual maximum water cover showed a fluctuating downward trend.

Dataset citations

Huichan Liu, Guojin He. Global 30-m annual maximum land surface water cover in 2000, 2005, 2010, 2015, 2021 (GAMLSW30), Beijing: International Research Center of Big Data for Sustainable Development Goals (CBAS), 2023. doi: 10.12237/casearth.640f007a819aec3f2b52a48c

References

Huichan Liu, Guojin He, Yan Peng, et al. 2021. Dynamic monitoring of surface water in the Tibetan Plateau from 1980s to 2019 based on satellite remote sensing images. Journal of Mountain Science, 18, 2833–2841 (2021). https://doi.org/10.1007/s11629-020-6482-8

Product URL

http://data.casearth.cn/thematic/GWRD_2023

QR code

Contact information

Huichan Liu, Associate Professor, hcliu@cbas.ac.cn Guojin He, Professor, gjhe@cbas.ac.cn

Citation and Disclaimer for Data Use

Global 30-m annual maximum land surface water cover

Global 8-day/250-m surface water extent dynamics from 2000 to 2020 (GSWED250_2000-2020)

Product summary

This product is designed to monitor the open surface water (called " surface water ") where the land surface is not blocked by vegetation and not frozen, including all types of water bodies such as rivers with a width greater than 250 meters and lakes and reservoirs with a surface area greater than 0.0625 km^2. With the high temporal resolution (8-day), this product can be used to accurately reflect changes in the distribution of surface water over time (called "water dynamics"). Land surface water dynamics is one of the most important indicators of changes in water resources. Accurate determination of land surface water dynamics is important for understanding the characteristics of the Earth system water cycle and its response to climate change and human activities. Such data products have important application values for water resources management.

Temporal

The product covers the period 2000–2020, with a temporal resolution of 8 days.

Geo Scope

The product covers the geographical area between 75° N–60° S latitude and 180° W–180° E longitude, with a spatial resolution of 250m.

support
SDGs

- SDG 6.6.1 Change in the extent of water-related ecosystems over time
- SDG 13.2.2 Total greenhouse gas emissions per year
- SDG 15.1.2 Proportion of important sites for terrestrial and freshwater biodiversity that are covered by protected areas, by ecosystem type

Global surface water dynamics in 2020

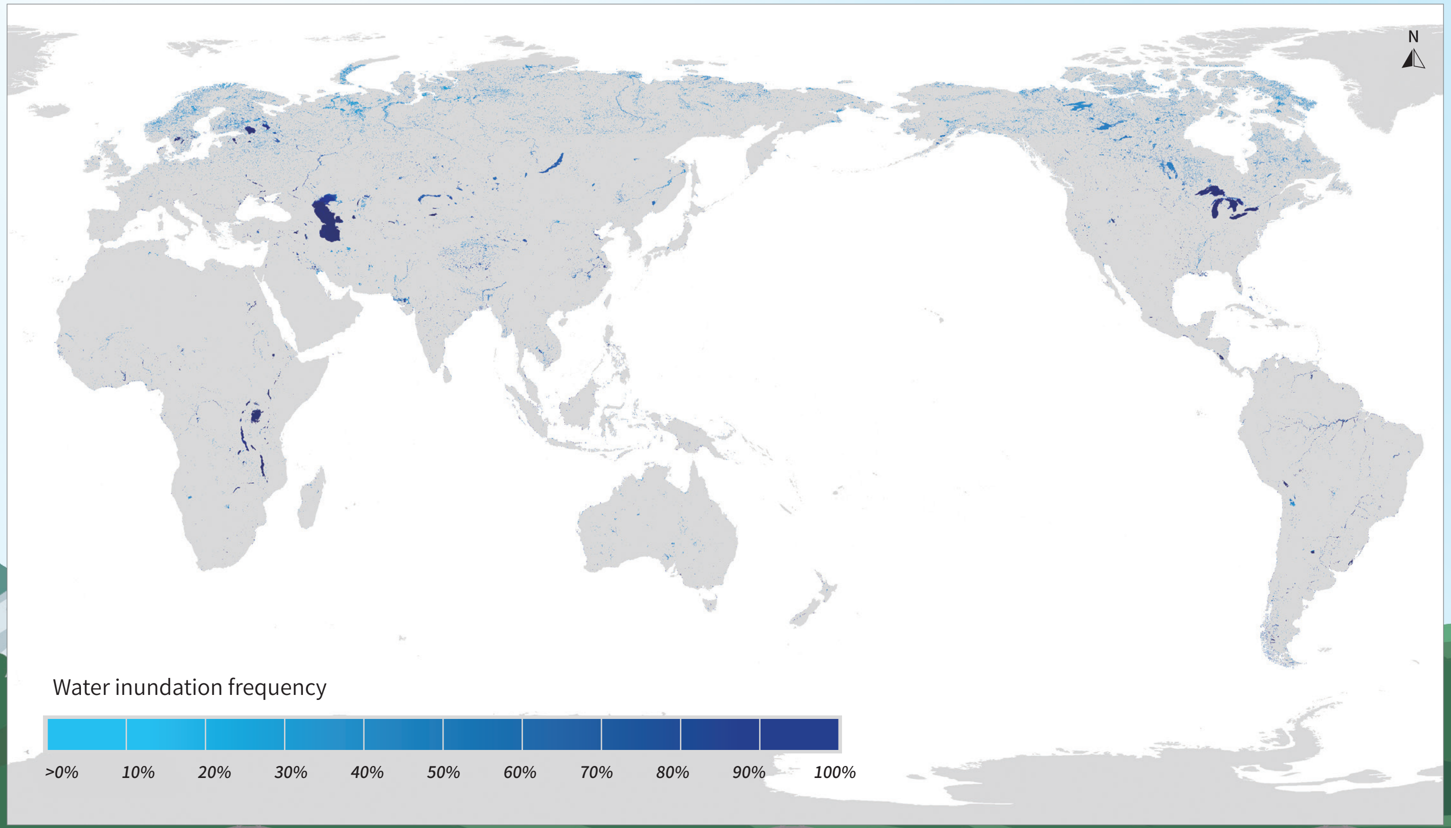

Methodology

The product was generated based on the remote sensing vegetation index threshold method, in combination with multi-source remote sensing data (Han & Niu, 2020).

The source data used to generate the product include MODIS-related data (MOD44W, MOD09Q1, MOD09A1, MOD13Q1, and MOD11A2) and topographic data (Shuttle Radar Topography Mission and Global 30 Arc-Second Elevation).

The global land area is first divided into 807 tiles of 5° ×5° latitude and longitude, and the 8-day MODIS NDVI data are used to determine the water surface extraction threshold for each 8-day of the year for each tile. The preliminary product of global surface water extent was then produced based on the spatiotemporal NDVI thresholds. Furthermore, the spatiotemporal filtering model and ancillary data were used to remove the influence of clouds, shadows, snow/ice and bare ground, and the dynamic distribution of global land surface water bodies was obtained at 8-day resolution.

Accuracy assessment

The product was validated by using 8687 spatially and temporally random water samples, with an overall accuracy of 96%. In addition, the water bodies extracted from Landsat OLI time series data in four different regions of the world (Dead Sea, Utah Lake, Qinghai Lake and Siling Lake) were compared with this product, and the results showed that the two were in good agreement (correlation coefficient greater than 0.9).

Product format

This product uses the WGS84 geographic coordinate system and longitude and latitude projection (EPSG: 4326). Data are stored in GeoTIFF format. Each annual product contains 807 spatial tile files, each tile file having a spatial extent of 5° ×5° latitude and longitude. Each tile file has 955 layers (bands), with a value of 1 for water bodies, 3 for snow/ice, 4 for land, 5 for mountain shadows, and 6 for clouds.

Analysis result

The analysis results showed that the total area of global surface water bodies (water area greater than 0.0625 km^2) ranged from 1.23 to 2.27 million square kilometers from 2000 to 2020. The maximum value of global water bodies was 2.27 million square kilometers in August 2000 and the minimum value was 1.23 million square kilometers in February 2014. The intra-annual variability of the global surface water area showed a non-significant decrease, indicating a slowdown in the intra-annual seasonal variability of global water bodies. Globally, there is a general increasing trend in the area of inland basins, such as in High Mountain Asia, the African Sahel and the Central American region. In contrast, surface water bodies in coastal basins generally showed decreasing trends, such as the basins in the northern Mediterranean, the Black Sea and Dead Sea in the Middle East, northwestern Australia, and the southern Africa.

Dataset citations

Zhenguo Niu, Qianqian Han. Global 8-day/250-m surface water extent dynamics from 2000 to 2020 (GSWED250_2000-2020), Beijing: International Research Center of Big Data for Sustainable Development Goals (CBAS), 2023. doi: 10.12237/casearth.640f00f4819aec3f2b52a499

References

Qianqian Han, Zhenguo Niu. 2020. Construction of the Long-Term Global Surface Water Extent Dataset Based on Water-NDVI Spatio-Temporal Parameter Set. Remote Sensing, 12, 2675. https://doi.org/10.3390/rs12172675

Product URL

http://data.casearth.cn/thematic/GWRD_2023

QR code

Contact information

Zhenguo Niu, Professor, zgniu@cbas.ac.cn   Qianqian Han, phD, qqhan@cbas.ac.cn

Citation and Disclaimer for Data Use

Global 500-m Forel-Ule Index product of large lakes from 2000 to 2021 (FUIGL500_2000-2021)

Product summary

The Forel-Ule Index (FUI), also known as the water color index, can be a useful indicator of overall water quality. It originates from the traditional Forel-Ule scale, which classifies the color of natural water into 21 scales ranging from dark blue to yellowish-brown. In generally, the lower the FUI, the cleaner the water; conversely, the higher the FUI, the more turbid the water.

Temporal

The product covers the period 2000–2021, with a temporal resolution of 1 year.

Geo Scope

The product covers 1,149 large lakes with a water surface area of more than 25 km^2 worldwide, with a spatial resolution of 500m.

support SDGs

6 CLEAN WATER AND SANITATION

SDG 6.3.2 Proportion of bodies of water with good ambient water quality

SDG 6.6.1 Change in the extent of water-related ecosystems over time

Remotely sensed Forel-Ule Index of global large lakes in 2020

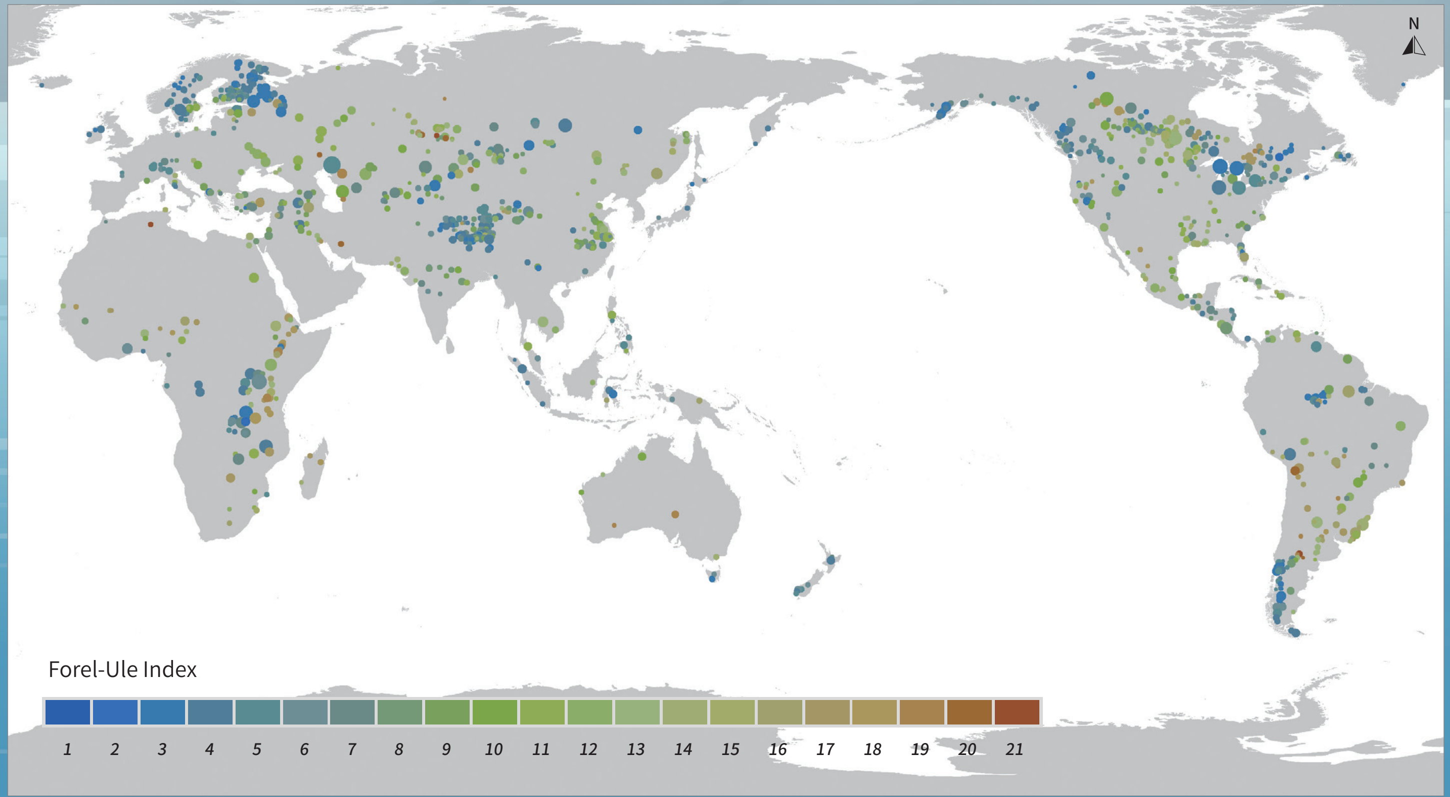

Global 500-m Forel-Ule Index product of large lakes

Methodology

The input data of this product are the 8-day composites of Terra MODIS land surface reflectance data. The generation of the product consists mainly of the following steps: (1) Extracting water distribution from the input MODIS data for large lakes with water area larger than 25 km^2 (Wang et al., 2018); (2) Making correction for water-leaving reflectance of the extracted water area; (3) Transforming the water-leaving reflectance data from RGB (red, green, and blue) color space to CIE (Commission Internationale d'Eclairage) color space, and then determining the FUI value according to the CIE color space coordinate lookup table (Wang et al., 2021); (4) Averaging the FUI values in summer every year (June–September in the northern hemisphere, and last December–March in the southern hemisphere), and finally obtaining the annual average FUI product of global large lakes from 2000 to 2021.

Accuracy assessment

The FUI product was validated using the in-situ measurements of water surface reflectance from 151 samples in 7 typical large lakes in Asia and America in concurrence with satellite images. FUI values calculated from the in-situ measurements of water surface reflectance were used as ground truth data to validate the FUI product. Comparison shows that the mean relative error of the FUI product is 6.5% and the overall accuracy of the FUI product is 93.5%.

Product format

This product uses the WGS84 geographic coordinate system and latitude/longitude projection (EPSG: 4326). The data are stored in GeoTIFF format. Each annual product is divided into spatial tiles, each tile having a spatial extent of 10° ×10° latitude and longitude. Each tile contains one data layer (band) with integers from 1 to 21 for the FUI scales and 0 for the background value.

Analysis result

The analysis results show that, the large lakes located in high latitude and high altitude generally have lower FUI, indicating relatively lower turbidity, while large lakes located in regions with high population density and high level of urbanization generally have higher FUI, indicating relatively higher turbidity. Since 2000, 34.8% of the large lakes have a significant decreasing trend in FUI values, indicating less turbidity of the water, mainly located in the cold temperate zone and the Qinghai-Tibet Plateau; while 7.2% of the large lakes have a significant increasing trend in FUI values, indicating more turbidity of the water, mainly located in arid regions.

Dataset citations

Shenglei Wang, Junsheng Li. Global 500-m Forel-Ule Index product of large lakes from 2000 to 2021 (FUIGL500_2000-2021), Beijing: International Research Center of Big Data for Sustainable Development Goals (CBAS), 2023. doi: 10.12237/casearth.640f00a8819aec3f2b52a492

References

Shenglei Wang, Junsheng Li, Wenzhi Zhang, et al. 2021. A dataset of remote-sensed Forel-Ule Index for global inland waters during 2000–2018. Scientific Data, 8, 20. https://doi.org/10.1038/s41597-021-00807-z

Shenglei Wang, Junsheng Li, Bing Zhang, et al. 2018. Trophic state assessment of global inland waters using a MODIS-derived Forel-Ule index. Remote Sensing of Environment, 217, 444-460. https://doi.org/10.1016/j.rse.2018.08.026

Product URL

http://data.casearth.cn/thematic/GWRD_2023

QR code

Contact information

Shenglei Wang, Assistant Professor, slwang@cbas.ac.cn Junsheng Li, Professor, jsli@cbas.ac.cn

Citation and Disclaimer for Data Use

Global 250-m algal bloom frequency of large lakes from 2000 to 2021 (ABGL250_2000-2021)

Product summary

The algal bloom defined in this product refers to the phenomenon of excessive growth of algae and the formation of algal scums on the water surface, which is expressed by the algal bloom frequency (unit: percentage). The algal bloom frequency refers to the ratio of the number of times is identified as an algal bloom to the number of valid observations per year in each pixel. Algal blooms have a major impact on the lake water quality and the safety of drinking water for local communities. Accurate information on the spatiotemporal dynamics of algal blooms in lakes is important for the water management policy making and the lake ecosystem assessment.

Temporal

The product covers the period 2000–2021, with a temporal resolution of 1 year.

Geo Scope

The product covers 161 large natural lakes with a water surface area of more than $500km^2$ around the world, with a spatial resolution of 250m.

support SDGs

SDG 6.3.2 Proportion of bodies of water with good ambient water quality

SDG 6.6.1 Change in the extent of water-related ecosystems over time

The frequency classification of algal blooms in global large lakes from 2000 to 2021

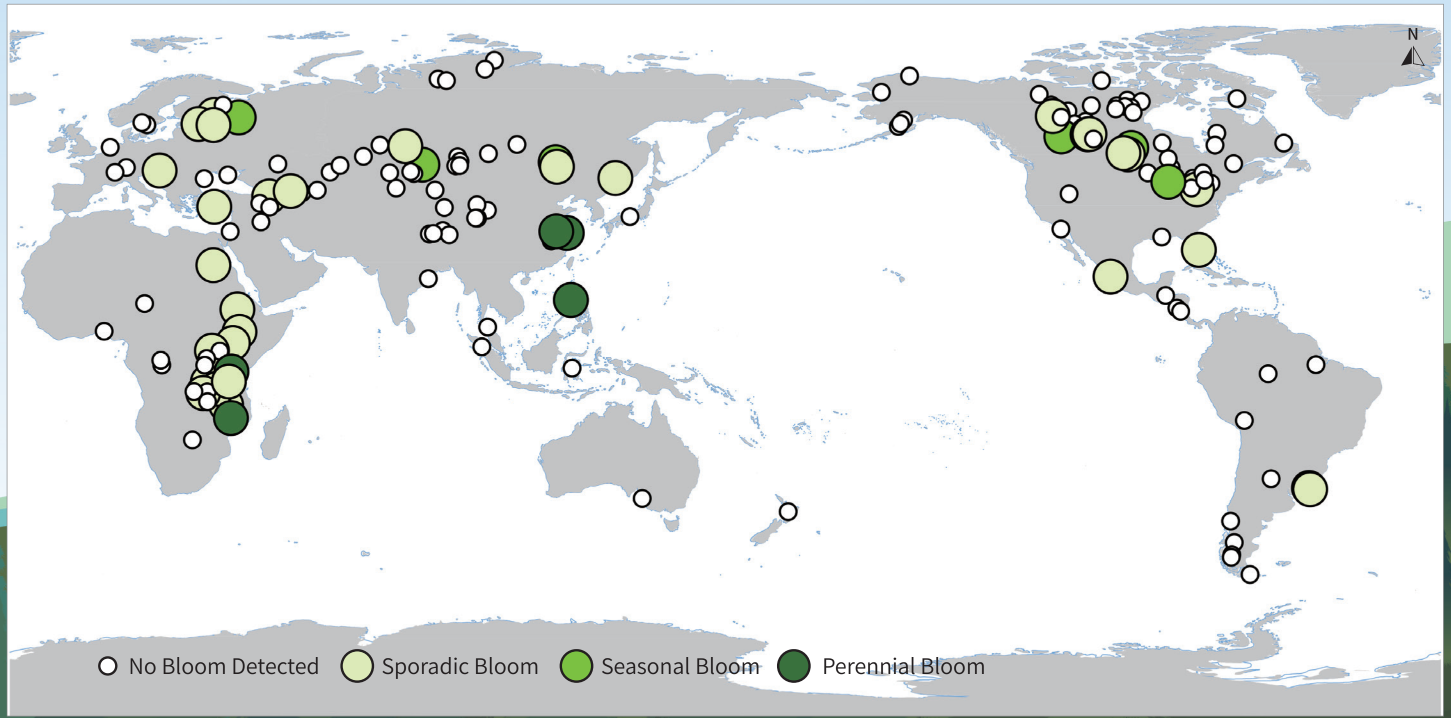

Global 250-m algal bloom frequency of large lakes

Methodology

This product used HydroLAKES dataset, MOD09GA/MOD09GQ surface reflectance products, MOD10A1 Normalized Difference Snow Index (NDSI) product, and MOD11A1 Land Surface Temperature (LST) product as data sources. First, a list of basic eutrophication information on global large lakes (> 500km^2) was compiled through literature review, data collection and Google search. Next, the above MODIS products and the HydroLAKES dataset were applied in Google Earth Engine (GEE) to calculate the Floating Algae Index (FAI) (Hu 2009), Cyanobacteria Macrophyte Index (CMI) and Turbid Water Index (TWI) (Liang et al., 2017) for each piexl in the lake. Subsequently, the NDSI and LST were used to identify and mask out pixels with ice. TWI and CMI were used to identify and mask the highly turbid water areas and aquatic vegetation areas. The inter-pixel gradients of the FAI images were calculated. The FAI threshold for extracting the algal bloom area was obtained by the maximum gradient method. The above procedures were applied to the cloud-free and noise-free FAI images from 2000 to 2021. Finally, the product of the algal bloom frequency of the world's large lakes was obtained by calculating the ratio of the number of times is identified as an algal bloom to the number of valid observations per year in each pixel (Duan et al., 2009; Ma et al., 2022).

Accuracy assessment

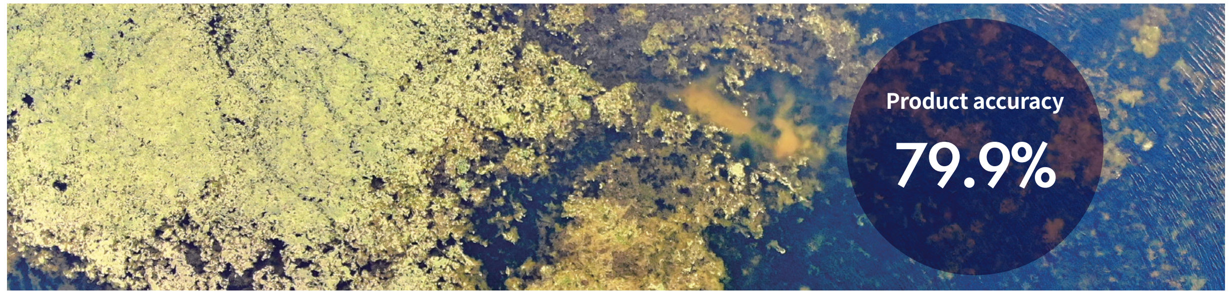

A total of 16 lakes on four continents were selected and the areas of algal bloom were extracted as the true value by visual interpretation of the original images. In addition, when compared with the published algal bloom data, this product was found to be generally consistent with the published data in terms of inter-annual variation of bloom area.

Product format

This product uses the WGS84 geographic coordinate system and latitude/longitude projection (EPSG: 4326). There are 22 files in total, each file containing 1 layer (band) corresponding to 1 year of data. The value in each pixel represents the ratio of the number of times is identified as an algal bloom to the number of valid observations per year in each pixel, in percentage (%) as the unit.

Analysis result

The analysis results showed that since 2000, 40 of the world's 161 large lakes experienced algal blooms, accounting for 24.8% of the total number of lakes monitored. The number of lakes with algal blooms, the area and frequency of algal blooms around

the globe have showed a significant increasing trend. The proportion of lakes with algal blooms was highest in the temperate zone (such as central Europe and the Asian plains), followed by the tropical zone (such as central Africa), and lowest in the arid zone (such as North Africa and western Asia). Lakes with perennial blooms occurred only in the tropical and temperate zones, and lakes with seasonal blooms only occurred in continental zone (such as high latitude regions in North America). The proportion of lakes with algal blooms was the highest in the temperate zone because the concentration of nutrients was higher in the temperate lakes due to denser population and the climate was more conductive for algae growth.

Dataset citations

Hongtao Duan, Jinge Ma. Global 250-m algal bloom frequency of large lakes from 2000 to 2021 (ABGL250_2000-2021), Beijing: International Research Center of Big Data for Sustainable Development Goals (CBAS), 2023. doi: 10.12237/casearth.640f00fd819aec3f2b52a4a1

References

Hongtao Duan, Ronghua Ma, Xiaofeng Xu, et al. 2009. Two-decade reconstruction of algal blooms in China's Lake Taihu. Environmental Science & Technology, 43(10), 3522-3528. doi: 10.1021/es8031852. PMID: 19544849

Jinge Ma, He Feng, Tianci Qi, et al. 2022. Thirty-Four-Year Record (1987–2021) of the Spatiotemporal Dynamics of Algal Blooms in Lake Dianchi from Multi-Source Remote Sensing Insights. Remote Sensing, 14(16), 4000. https://doi.org/10.3390/rs14164000

Chuanmin Hu. 2009. A novel ocean color index to detect floating algae in the global oceans. Remote Sensing of Environment, 113(10), 2118-2129. https://doi.org/10.1016/j.rse.2009.05.012

Qichun Liang, Yuchao Zhang, Ronghua Ma, et al. 2017. A MODIS-based novel method to distinguish surface cyanobacterial scums and aquatic macrophytes in Lake Taihu. Remote Sensing, 9(2), 133. https://doi.org/10.3390/rs9020133

Product URL

http://data.casearth.cn/thematic/GWRD_2023

QR code

Contact information

Hongtao Duan, Professor, htduan@cbas.ac.cn Jinge Ma, phD, jgma@cbas.ac.cn

Citation and Disclaimer for Data Use

Monthly 0.5° groundwater storage change in Africa from 2003 to 2020 (GWS-AF05_2003-2020)

Product summary

The monitoring objective of this data product is the groundwater storage change, which refers to the monthly anomaly relative to the 2003–2020 mean and is expressed in equivalent water height (unit: mm). Groundwater storage change is a key indicator reflecting the change in groundwater quantity in aquifers.

This product provides essential data to support the sustainable management of groundwater resources.

Temporal

The product covers the period 2003–2020, with a monthly interval.

Geo Scope

The product covers the geographical area between 36.75° N–34.25° S latitude and 16.75° W–50.75° E longitude.

support SDGs

6 CLEAN WATER AND SANITATION

SDG 6.4.2 Level of water stress: freshwater withdrawal as a proportion of available freshwater resources

SDG 6.5.1 Degree of integrated water resources management

SDG 6.6.1 Change in the extent of water-related ecosystems over time

The long-term (2003–2020) trends in monthly groundwater storage change in Africa

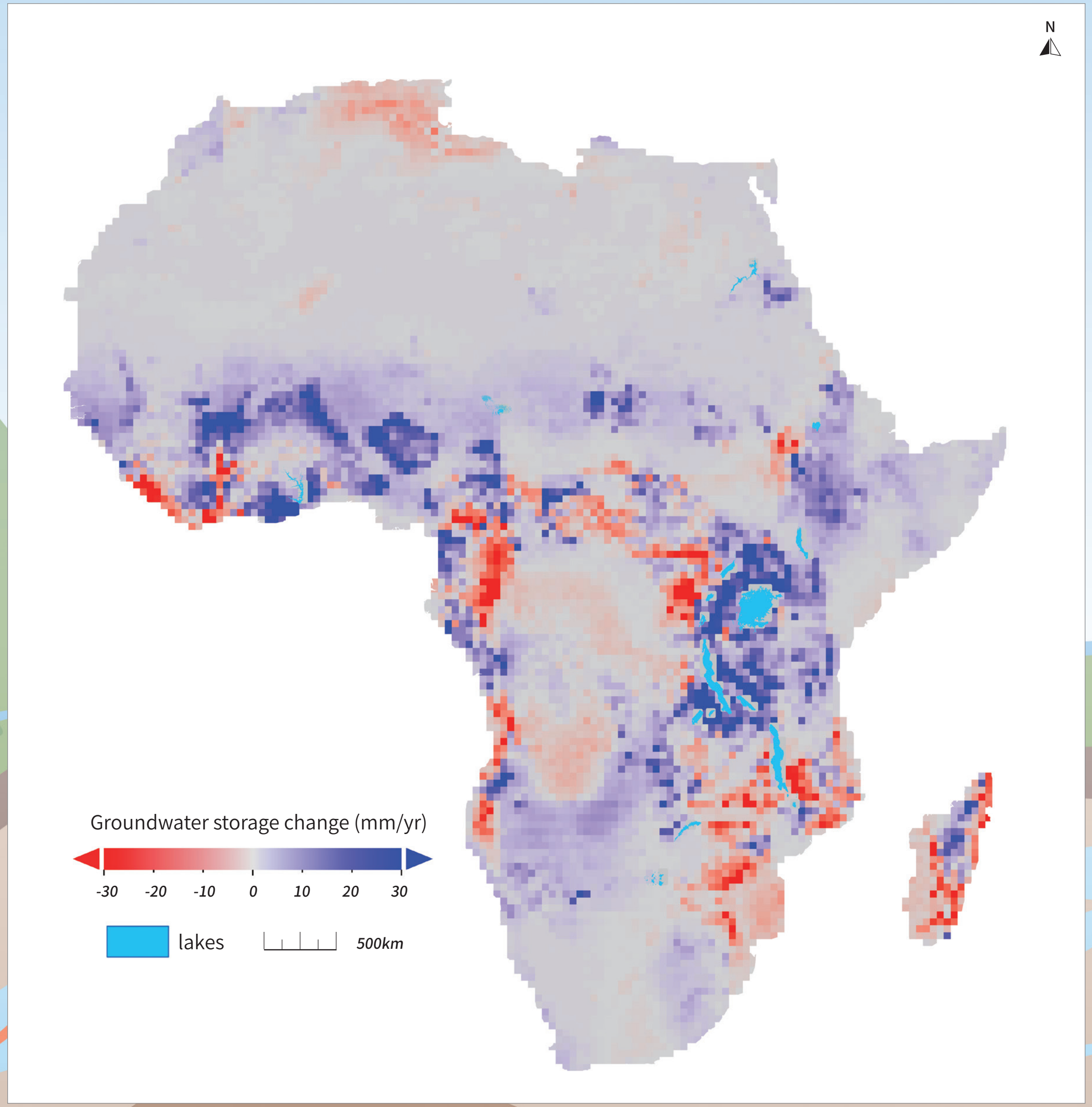

Methodology

The data used are spherical harmonic coefficient from GRACE (Gravity Recovery and Climate Experiment) & GRACE Follow-On and model simulations from CLSM (Community Land Surface Model) v2.2. GWS05_AF_2003-2020 was produced using the coordinated forward modeling (CoFM) method, which uses model simulations to constrain the GRACE mass change signal and reduce bias and leakage errors at the grid scale. This overcomes the limitations of lack of effective spatial constrains in the conventional forward modeling. The monthly groundwater storage change can be calculated by multiplying the iteratively updated aquifer storage coefficients and simulated groundwater level.

The non-groundwater storage compartments, including soil water, surface water, snow water equivalent and canopy water, were first subtracted from the terrestrial water storage change observed by GRACE & GRACE Follow-On without any corrections for bias/leakage errors. These errors were then corrected by the CoFM by iteratively updating the aquifer storage coefficients, which were finally used together with the simulated groundwater levels to estimate the monthly groundwater storage change on a 0.5° grid scale.

Accuracy assessment

The product was evaluated against groundwater levels observed in-situ from 268 monitoring wells over the period 2003–2020 in Africa. The estimated groundwater storage change was compared with the in-situ groundwater levels to calculate the correlation between the two at monthly intervals. The results show that the average regional correlation is 67.3%. However, it should be noted that there are large uncertainties in this type of evaluation, as groundwater level change is different from groundwater storage change. In addition, the spatial distribution and the number of monitoring wells can strongly influence the correlation between the two.

Product format

This product uses the WGS84 geographic coordinate system and longitude and latitude projection (EPSG: 4326). Data are stored in GeoTIFF format. The spatial resolution is 0.5° . There are 215 files in total, each file containing groundwater storage change for each month. The unit is mm/month.

Analysis result

The analysis results showed that groundwater storage in Africa increased at a rate of 1.47 mm/yr during the period 2003-2020, with notable differences in the spatial distribution of the rates. The area with significant ($p<0.05$) increasing and decreasing trends in groundwater storage accounted for 27% and 37% of Africa's land area, respectively. The increasing trends were mainly found in the Niger River Basin and the East African Plateau, while the North of the Sahara, the Congo River Basin, and the Lower Zambezi River Basin are the main areas with decreasing trends. The divergent spatial distribution is mainly driven by changes in precipitation and regional groundwater abstraction. The results highlight the importance of groundwater management for sustainable development in arid areas such as the northern Sahara, and the need to mitigate drought-induced water scarcity in humid areas such as the Congo River Basin.

Dataset citations

Yun Pan. Monthly 0.5° groundwater storage change in Africa (GWS-AF05_2003-2020), Beijing: International Research Center of Big Data for Sustainable Development Goals (CBAS), 2023. doi: 10.12237/casearth.640f0104819aec3f2b52a4a8

References

Yun Pan, Chong Zhang, Huili Gong, et al. 2017, Detection of human-induced evapotranspiration using gravity satellite observations in the Haihe River Basin of China. Geophysical Research Letters, 44(1): 190-199. https://doi.org/10.1002/2016GL071287

Product URL

http://data.casearth.cn/thematic/GWRD_2023

QR code

Contact information

Yun Pan, Professor, yunpan@cbas.ac.cn

Citation and Disclaimer for Data Use

Monthly 0.5° groundwater storage change in Africa

International Research Center of Big Data for Sustainable Development Goals
Address: No. 9 Dengzhuang South Road, Haidian District, Beijing
Postal code: 100094
Telephone: +86 10 82177601
E-mail: datasharing@cbas.ac.cn
Map Approval Number: GS （2023）0434